Methanol electrosynthesis from CO_2 at Cu_2O/ZnO prompted by pyridine-based aqueous solutions

Jonathan Albo[a, c*], Garikoitz Beobide[b], Pedro Castaño[a] and Angel Irabien[c]

[a]*Department of Chemical Engineering, University of the Basque Country, Apdo. 644, 48080, Bilbao, Spain*

[b]*Inorganic Chemistry Department, University of the Basque Country, Apdo. 644, 48080, Bilbao, Spain*

[c]*Department of Chemical & Biomolecular Engineering, University of Cantabria, Avda. Los Castros s/n, 39005 Santander, Spain*

[*]Corresponding author; e-mail: jonathan.albo@unican.es

Abstract

In this study we examine the electrochemical-driven reduction of CO_2 to methanol at Cu_2O/ZnO gas diffusion electrodes in soluble pyridine-based electrolytes at different concentrations. The process is evaluated first by cyclic voltammetric analyses and then, for the continuous reduction of CO_2 in a filter-press electrochemical cell. The results showed that the use of pyridine-based soluble co-catalysts lowered the overpotential for the electrochemical reduction of CO_2, enhancing also reaction performance (i.e. reaction rate and Faradaic efficiency). Reaction outcome is discussed on the basis of the role that N-ligands play on the mechanism and the inductive effect caused by the electron-releasing or electron-withdrawing substituents of the aromatic ring.

In particular, the maximum methanol formation rate and Faradaic efficiency reached at the 2-methylpyridine (with electron-releasing substituents)-based system with a pH of 7.6 and an applied current density of j= 1 mA·cm^{-2} were r= 2.91 µmol·m^{-2}·s^{-1} and FE= 16.86%, respectively. These values significantly enhance those obtained in the absence of any molecular catalyst (r= 0.21 µmol·m^{-2}·s^{-1} and FE= 1.2%). The performance was further enhanced when lowering the electrolyte pH by adding HCl (r= 4.42 µmol·m^{-2}·s^{-1} and FE= 25.6% at pH =5), although the system showed deactivation in the long run (5 h) which appears largely to be due to a change in product selectivity of the reaction (i.e. formation of ethylene).

Keywords: Electrochemistry, CO_2 reduction, pyridine-based molecular catalysts, copper oxide, methanol

1. Introduction

The idea that CO_2 can be captured [1-3] and reconverted to fuels in a Carbon Capture and Utilisation (CCU) approach, sounds like a perfect solution that potentially could help to solve global warming and energy shortage issues [4, 5]. Among the available technologies for the activation and conversion of CO_2 into value-added chemicals [6], the electrocatalytic alternative is appealing since it could enable an economically competitive industrial production of CO_2-based fuels by using renewable energy [7, 8].

Moreover, from the spectrum of possible CO_2-reduced species, the formation of methanol (CH_3OH) is of great interest since it is liquid at ambient conditions and can be readily integrated into the existing liquid fuel transportation infrastructure [9, 10]. However, an effective and selective production of CH_3OH (with 6 exchanged e^- required) by electrochemical methods is a chemical challenge that still remains unsolved. Despite the significant contributions that have been recently made in this reaction [9, 11-13], most of the CO_2 electroreduction reports have been largely confined to 2 e^- products such as CO and formate (HCOOH) and, in many cases, with low productivities. Besides, even though proton-coupled electron transfers to CO_2 are thermodynamically facile, these reactions require large overpotentials [9]. In order to help solving those limitations, organic molecules have been found to be beneficial to promote the electrochemical reduction of CO_2 [14, 15]. In particular, nitrogen-containing heterocycles such as pyridine (Py) appear to lower overpotentials (indicating lower reaction barriers) and increase Faradaic efficiencies (indicating higher selectivities toward CO_2 reduction products) in electrochemical CO_2 conversion reactions as largely demonstrated by Bocarsly et al. [16-22]. Their first results evidenced that CO_2 is catalyzed at hydrogenated Pd electrodes in 10 mM aqueous Py solutions [19, 22]. CH_3OH was detected with efficiencies up to 30% at overpotentials of uniquely ~200 mV [22]. Py was found to act as electron shuttle implying the formation of a carbamate as intermediate during the electron transfer to CO_2 [19]. In 2008, the same group exported this chemistry to a p-GaP photoelectrochemical cell to yield 96% Faradaic efficiency (*FE*) for CH_3OH. They showed evidence of the key role of Py to catalyze the selective formation of CH_3OH from CO_2 in a series of one-electron steps at underpotentials of about 300 mV [21]. Based on the interesting results for the electro-and-photoelectrocatalytic CO_2 reduction using Py developed by the group of Bocarsly, recent reports from other groups have been advancing on the application of Py-based molecular catalyst [23-29], demonstrating the benefits of using molecular catalysts for the reduction of CO_2 to CH_3OH.

While the mechanisms of the reduction process seem to be still subject of debate, the results clearly show that the identity of the soluble heterocycle and the metal electrode influences the yield and product selectivity of the reaction [23, 30-34]. For example, the use of Py with a p-GaP or a Pt cathode results in selective CH_3OH formation, while Py with a Fe-pyrite cathode favours HCOOH production [15, 17, 22]. Among the available catalytic materials, copper has been found to be unique to synthesize CH_3OH and >C1 hydrocarbons, such as ethanol and propanol [11-13, 35-37]. The performance of this metal, however, generally implies large overpotentials and low selectivities [38]. Nevertheless, copper(I) oxide surfaces (i.e. Cu_2O) present both intermediate hydrogen overpotentials and CO adsorption properties, which allows higher CH_3OH yields in aqueous solutions to be produced [12, 13, 39-41]. Moreover, our previous work [13] demonstrated that ZnO is able to stabilize Cu_2O in the hydrogenation reaction, maintaining the stability of the catalyst for longer reaction times.

Therefore, with the present study we sought to address the use of Py-based aqueous solutions for CO_2 conversion at Cu_2O/ZnO-based working electrodes. Previous works have pointed that N-donor ligands like pyridine play a crucial role in the electron transfer to CO_2 by forming a carbamate intermediate. Herein, a handful of pyridine derivatives were used in this study in order to assess the inductive effect caused by electron-releasing (*I*+) and electron-widthdrawing (*I*–) substituents into the overall reaction outcome. Precisely, we selected unsubstituted pyridine as reference and 2-methylpyridine, 4-ethylpyridine, 2,4,6-trimethylpyridine, 2-chloropyridine, and 4,4'-bipyridine as representative cases for *I*+ and *I*– effect. Influence of parameters such as Py type and its concentration was preliminarily addressed by cyclic voltammetry. Thereafter, continuous reduction of CO_2 to CH_3OH was conducted in a filter-press electrochemical cell at low current densities (j= 0.01 - 5 $mA{\cdot}cm^2$) in a pH range from ca. 7.6 to 4.

2. Materials and methods

2.1. Py-based molecular catalysts

Pyridine (Py, 99%), 2-methylpyridine (2mPy, 98%), 4-ethylpyridine (4ePy, 98%), 2,4,6-trimethylpyridine (246tmPy, 99%), 2-chloropyridine (2ClPy, 99%), and 4,4'-bipyridine (44biPy, 99%) of reagent grade were used as commercially obtained. Figure 1 depicts the selected pyridines, together with the pKa values of the corresponding pyridinium. It must be noted that the pKa value can be correlated with inductive effect of the ring substituents. When compared to the unsubstituted Py, the alkyl derivatives (2mPy, 246tmPy and 4ePy) display an electron-releasing effect towards the N atom, making it a more basic position (i.e. a greater pKa of the pyridinium). 44biPy and 2ClPy exhibit somewhat lower and markedly lower pKa values according to their mild and strong electron-withdrawing effects. These features will be considered in the discussion section, as they are also closely related to the ability of the pyridinic ring to mediate the electron transfer through the formation of a carbamate intermediate by the nucleophilic addition to CO_2.

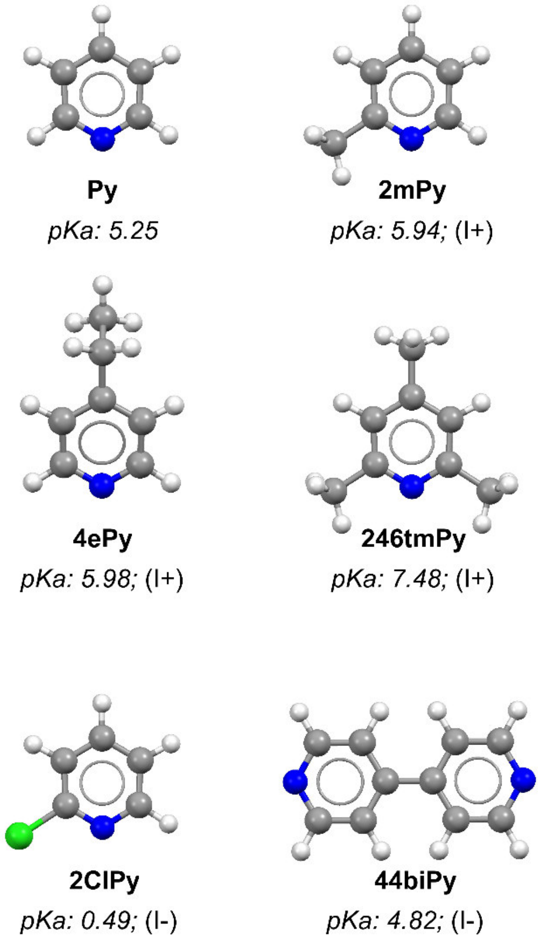

Figure 1. Selected pyridines (colour codes: C grey, H white, N blue, and Cl green) including pKa values of the corresponding pyridinium. Nature of the inductive effect in parentheses.

2.2. Cyclic voltammetry characterization

The electrochemical behaviour was evaluated with a PGSTAT 302N potentiostat (Metrohm, Autolab B.V.) under GPES software control employing a conventional three electrode electrochemical cell. A glassy carbon and Ag/AgCl (sat. KCl) were used as a counter and reference electrode, respectively. Portions of the Cu_2O/ZnO-based materials were used as cathodes. The aqueous electrolyte (0.5 M $KHCO_3$) containing the different molecular catalysts at different concentrations (i.e. 10, 25 and 50 mM) was saturated with ultrapure CO_2 (99.99%) by bubbling for 20 min before the tests. The current-voltages curves were obtained with a scan rate of 50 $mV \cdot s^{-1}$ at potentials ranging from 0 to -1.2 V vs. Ag/AgCl. Current density is expressed as the total current divided by the geometric surface area, A, of the electrodes.

2.3. Electrochemical cell for CO_2 reduction

The continuous electrochemical measurements for CO_2 reduction were carried out in a filter-press electrochemical cell (Micro Flow Cell, ElectroCell A/S) at ambient conditions. A cation exchange membrane (Nafion® 117) separated the cathode and anode compartments of the cell. The membrane presented a phase-segregated structure that allows the selective transport of H^+ ions from the anode to the cathode chamber with a low permeability to CH_3OH [42]. A platinised titanium electrode was used as a counter electrode and Ag/AgCl (sat. KCl), assembled close to the cathode, was used as reference electrode. The Cu_2O/ZnO-catalyzed carbon papers were employed as working electrodes (A= 10 cm^{-2}). The preparation of the Cu_2O/ZnO electrodes has been described in detail in our previous works [12, 13]. Basically, Cu_2O (Sigma Aldrich, particle size < 5 µm, 97% purity) and ZnO particles (ACROS organic, < 45 µm, 99.5%) were mixed with a Nafion® dispersion 5 wt.% (Alfa Aesar) and isopropanol, IPA (Sigma Aldrich), with a 70/30 catalyst/Nafion mass ratio and a 3% solids (catalyst + Nafion). The ink was airbrushed onto a porous carbon paper (TGP-H-60, Toray Inc.) to form a gas diffusion electrode (GDE) with a catalytic loading of 1 mg·cm^{-2}. All electrodes were dried and rinsed with deionised water before use.

The filter-press electrochemical system possesses three inputs (catholyte, anolyte and CO_2 separately) and two outputs (catholyte-CO_2 and anolyte). The GDE cell configuration allows the electroreduction of CO_2 supplied directly in gas phase [12, 43, 44]. The cathode side of the reactor was fed with CO_2 gas (99.99%) with a flow/area ratio of Q_g/A= 20 ml·min^{-1}·cm^{-2}, adjusted by a rotameter. A 0.5 M $KHCO_3$ (Panreac, >97% purity) aqueous solution containing different concentrations of the Py-based molecular catalysts (i.e. 10, 25 and 50 mM) was used as catholyte. The anolyte was a 0.5 M $KHCO_3$ aqueous solution. Prior to the experiments, the aqueous electrolyte was saturated with CO_2 by bubbling for 20 min. The pH of the saturated solution was measured with a pH-meter PH 25 (Crison, PAIS). The pH before the tests was adjusted to 4, 5 and 6 by adding HCl (Panreac, 37%).

The electrolytes were pumped from catholyte and anolyte tanks to the cell by two peristaltic pumps (Watson Marlow 320, Watson Marlow Pumps Group) at a flow rate of Q_e/A= 1 ml·min^{-1}·cm^{-2}. The experiments were performed at galvanostatic conditions in a current density range of j= 0.05 - 5 mA·cm^{-2}, using an AutoLab PGSTAT 302N potentiostat (Metrohm, Autolab B.V.) The experimental time was 90 min, where pseudo-stable conditions are reached [12, 13]. Liquid samples were taken every 15 min from the catholyte tank.

The concentration of products in each sample was analysed by duplicate in a headspace gas chromatograph (GCMS-QP2010 Ultra Shimadzu) equipped with a Flame Ionization Detector (FID). Compounds were separated on a DB-Wax 30 m x 0.25 mm x 0.25 µm column, with an injection and detector temperature of 250 ºC and 270 ºC, respectively. Helium was used as a carrier gas at a flow rate of 50 $ml \cdot min^{-1}$. The identification of obtained products was further confirmed by headspace gas chromatography-mass spectrometry (GCMS-N5975B) using a 60 m x 250 µm x 1.40 µm DB-624 capillary column. An averaged concentration was obtained for each point from the performance of three separate runs with an experimental error less than 17.3%.

The performance of the process is evaluated by the rate of CH_3OH production, *r* (i.e. CH_3OH obtained per unit of cathode area and time), and the *FE* (i.e. selectivity of the reaction to produce CH_3OH). *FE* is calculated assuming that 6 e^- are required per molecule of CH_3OH.

3. Results and discussion

3.1. Cyclic voltammetric analyses

Figure 2a reveals the current-voltage response after 5 electrochemical scans for the Cu_2O/ZnO GDEs in a CO_2-saturated 0.5 M $KHCO_3$ aqueous solution, and the response upon adding 25 mM concentration of 2mPy in the electrolyte solution. This Py-based co-catalyst was firstly selected due to its ability to significantly reduce the activation overpotential (i.e. its role in the activation energy due to electron transfer) for CO_2 reduction [45]. The results are compared to those responses obtained at a Cu plate. To further analyse the activity for CO_2 reduction, Figure 2b shows the curves for Cu_2O/ZnO and Cu electrodes under CO_2 and N_2 saturation. Current densities, *j*, are normalized to the geometric area (A) of the electrodes.

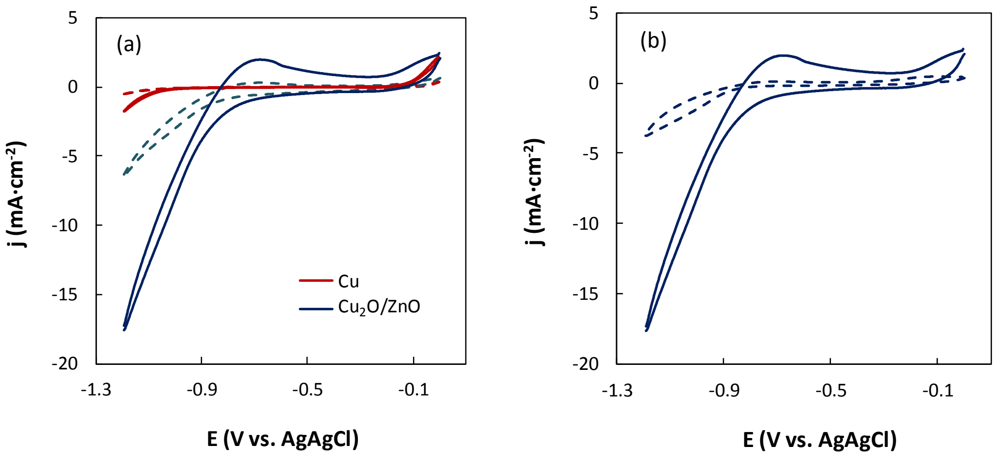

Figure 2. Cyclic voltammograms for: (a) Cu_2O/ZnO and Cu-based systems in CO_2-saturated 0.5 M $KHCO_3$ aqueous electrolytes in the presence and absence (dotted line) of 2mPy (25 mM) and, (b) Cu_2O/ZnO in CO_2 and N_2 (dotted line) saturated 0.5 M $KHCO_3$ + 2mPy (25 mM) solution.

Figure 2a shows that higher activities are reached for both Cu-based catalysts by employing Py-based molecular co-catalysts, as denoted by the large differences between voltammetry profiles in the absence/presence of 2mPy solubilised in the electrolyte. In fact, a very remarkable enhancement can be obtained in case of incorporating 25 mM of 2mPy in the Cu_2O/ZnO-based system, denoting the synergic co-catalytic effect of copper oxide species and Py in the activity response, in contrast with the restricted improvements at the Cu plate in the absence/presence of the molecular catalyst.

The main characteristic of the voltammograms is a reduction process starting at around -0.8 V vs. Ag/AgCl, which can be initially associated with the reduction of CO_2 and partial formation/decomposition of the oxides at the electrode surface. The oxidative peak at -0.7 V in the reverse scan of Cu_2O/ZnO curves might be initially assigned to the transition of remaining Zn to ZnO. However, the peak remains after the fifth scan, and so it probably has more to do with the formation of oxidized subproducts in the CO_2 reduction reaction. In addition, the curves in Figure 2b show that in the presence of both, 2mPy and CO_2, a substantial enhancement of the reduction wave, in comparison to that response in a N_2-saturated solution, was observed at more negative potentials than -1 V. Thus, this reduction peak is mainly attributed to CO_2 reduction rather than the oxidation-reduction of the catalytic materials. In fact, the reduction response occurs at around 200 mV lower overpotential in the presence of pyridine (compared to the system with a CO_2-saturated electrolyte without 2mPy). This denotes the important co-catalyst and synergic effect of 2mPy in the reduction of CO_2.

For the sake of evaluating the effect of the electron-releasing (*I*+) or electron-withdrawing (*I*-) character on CO_2 reduction activity, cyclic voltammograms were acquired for the other Py derivatives (i.e. 4ePy, 246tmPy, 2ClPy, 44biPy) in a concentration of 25 mM (Figure 3a). The results are compared to the electrochemical activity of unsubsituted Py as a reference. Besides, Figure 3b shows the effect of adding different concentrations of 2mPy (i.e. 10, 25 and 50 mM) in the CO_2 reduction response.

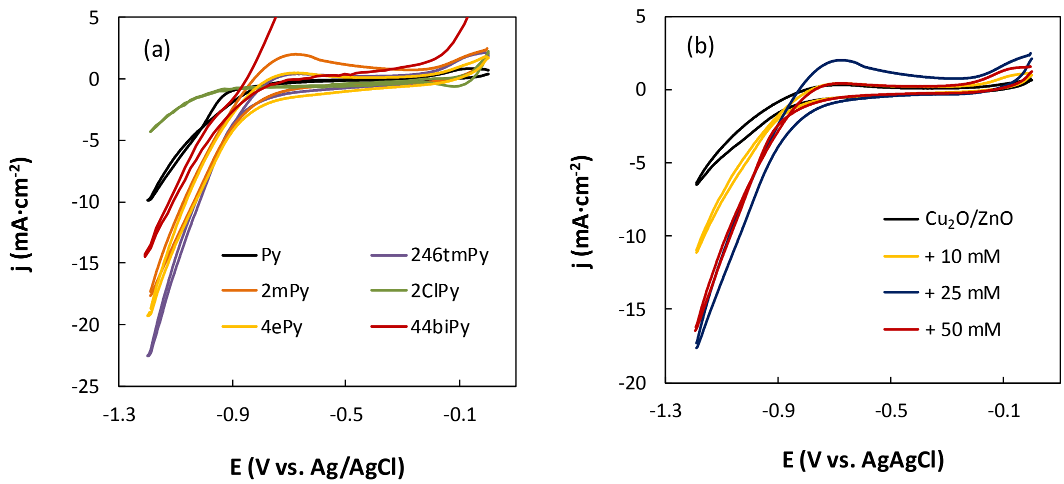

Figure 3. Cyclic voltammograms for Cu_2O/ZnO GDEs in a 0.5 M $KHCO_3$ aqueous solution containing: (a) 25 mM of the different Py-based molecular catalyst and, (b) different concentrations of 2mPy molecular catalyst (i.e. 10, 25 and 50 mM).

Compared to the reference Py, substituted ones show accused shifts on either onset of the reduction wave (i.e. lower activation overpotential) and its intensity. The lowering of the overpotential observed for 2mPy, 4ePy and 246tmPy can be rationalized by the electron releasing short alkyl groups (*I*+ effect). This makes the Py-N atom a better σ-donor and thus, more prone to form the carbamate through an addition reaction to the electrophilic C atom and, ultimately, to transfer the electron to CO_2.

On the contrary, the presence of a strong inductively electron-withdrawing group (*I*– effect) on the *orto* substituted 2ClPy, worsens σ-donor ability of N atom and hinders somewhat the formation of the carbamate and the resulting electron transfer. As a result, its voltammogram reveals a reduced current intensity and a shift towards greater overpotentials compared to referential Py. In the case of 44biPy, despite a slight worsening of the activity might be expected according to its moderate *I*– effect, its onset is somewhat lower than that of Py. Such behaviour might be attributed to the presence of two aromatic rings and two equivalent σ-donor N-atoms per molecule ready to transfer two electrons. It is noticeably that the marked oxidation peak found for the voltammogram measured in presence of 44biPy points to the formation and subsequent oxidation of reduced intermediates different to those rendered by other pyrdinic co-catalysts (i.e. a change in selectivity). This fact can be also related to the ability of 44biPy to promote 2 e- transfer which would imply mechanistic changes (see Figure S1 in Supplementary information). In any case, apart of influencing in the CO_2 reduction, it must be considered that Py ring mediated electron transfer prompts also the catalytic generation of hydrogen [46], being also responsible of the reduction wave behaviour. This process follows also the above described trend, as the *I*+ effect caused by electron releasing groups leads to more basic N atom (higher pKa of the corresponding pyridinium), resulting in a molecular catalyst more prone to bind a proton and transfer the electron.

Moreover, Figure 3b demonstrated that with increases in Py ions in the solution, the catalytic current-response is enhanced up to a concentration of 25 mM. Further increases in concentration did not lead to higher voltammetric responses. Hence, the redox CO_2 reaction is limited by the high concentration of Py, suggesting that CO_2 has become the limiting reagent as the concentration of Py increases [18, 26].

3.2. Filter-press electrochemical cell

To further explore the performance of these co-catalysts, Table 1 presents the data for the continuous transformation of CO_2 in the filter press electrochemical cell equipped with a Cu_2O/ZnO GDE and the Py derivatives tested at different concentrations (i.e. 10, 25 and 50 mM) in the supporting electrolyte (0.5 M $KHCO_3$). The results are compared with those obtained in the absence of any Py molecular catalyst. The pH of the electrolytes ranged from 6.8 to 7.6 on dependence of the Py-based co-catalyst applied. The analysis is carried out in terms of *r* and *FE* at a low current density (j= 1 $mA \cdot cm^{-2}$) where a better CO_2 electroreduction performance is expected in Py-based CO_2 co-catalyzed reactions [45].

The electroreduction process led to CH_3OH formation, with also traces of C_2H_5OH, in accordance to previous results at copper oxides surfaces [9, 21, 22] and recent reports on the application of pyridines for CO_2 electroreduction [27-29]. No other liquid products were detected. Control experiments for the reduction of CO_2 at low overpotentials catalyzed by the carbon paper (without sprayed Cu_2O/ZnO particles) did not produce any measurable liquid product.

Table 1. *r* and *FE* at Cu_2O/ZnO in the presence/absence of Py-based co-catalysts at different concentrations. j= 1 mA·cm^{-2}, Q_e/A= 1 ml·min^{-1}·cm^{-2}, Q_g/A= 20 ml·min^{-1}·cm^{-2}.

***Molec. Catalyst* (substituents)**	***Py conc.*, mM**	***E*, V vs. Ag/AgCl**	***r*, µmol·m^{-2}·s^{-1}**	***FE*, %**
-	-	-1.35	0.21	1.2
	10	-1.21	2.6	15.06
Py	25	-1.24	2.24	12.95
	50	-1.17	0.94	5.42
	10	-1.03	2.91	16.86
2mPy (*I*+)	25	-1.12	1.98	11.44
	50	-1	1.46	8.43
	10	-1.02	1.35	7.83
4ePy (*I*+)	25	-0.95	1.2	6.93
	50	-1.14	0.73	4.22
	10	-0.94	2.18	12.65
246tmPy (*I*+)	25	-0.99	2.24	12.95
	50	-1.03	1.51	8.73
	10	-1.41	0.73	4.22
2ClPy (*I*-)	25	-1.41	0.78	4.52
	50	-1.15	0.42	2.41
	10	-1.16	0.26	1.51
44biPy (*I*-)	25	-1.21	0.21	1.20
	50	-1.19	0.16	0.90

The results indicated that by employing Py-based co-catalysts, an enhancement in CH_3OH formation rates was observed in all cases, with values in general notably higher than those obtained at Cu_2O/ZnO GDEs in the absence of Py (r= 0.21 µmol·m^{-2}·s^{-1}) independently of the Py concentration applied. Besides, the cathodic voltages were in general more positive in case of adding Py-based molecular catalysts than those results in the absence of Py, being in concordance with the role that Py co-catalysts play in the electron transfer. For example, at an applied constant current of j= 1 mA·cm^{-2} (E=- 1.03 V vs. Ag/AgCl), an averaged *FE* for CH_3OH formation of 16.86% was observed with 2mPy (10 mM) as co-catalyst. Significantly higher voltage (E= -1.35 V vs. Ag/AgCl) was required under similar conditions in the absence of Py and only a *FE*= 1.2% was achieved. Moreover, the relative overpotential lowering follows the same trend that the one observed from cyclic voltammetric analyses (Figure 3a), according to the inductive effect caused by the substituents (see discussion in Section 3.1). Only 2ClPy shows an overpotential comparable to that provided by the Cu_2O/ZnO in the absence of co-catalyts, indicating that electron-withdrawing effect caused by the Cl^- substituent renders Py ring less active towards electron transfer (see above discussion).

As a rule, the lower voltages required in the Py-based co-catalysts are consistent with the faster kinetics to produce CH_3OH. The enhanced production rate is evident from comparison of r= 2.91 μmol·m^{-2}·s^{-1} obtained at 2mPy (10mM)-based system, which is an order of magnitude higher than r= 0.21 μmol·m^{-2}·s^{-1} in the absence of Py. Therefore, Py-based co-catalysts are able to reach higher r and FE at lower cathode potentials. Despite the relative low yields, the FE results are comparable to recent results (4-35%) for the use of pyridinium (protonated Py) and related aromatic nitrogen-heterocycles as electrocatalysts for CH_3OH production [28, 29, 47-49]. Despite Py derivatives cause, in general, an improvement in r and FE, the results do not match the expectations considering only the inductive effect. For instance, the overpotential reduction caused by $I+$ substituents is not strictly correlated with the CH_3OH production rate and Faradaic efficiency, since 4ePy and 246tmPy co-catalysts, possessing electron-releasing groups, reduce the overpotential with respect the unsubstituted Py, but lead to slightly worse r and FE values, which is probably due to the complexity of the multiple steps involved, stability of the intermediates and the formation of non-liquid subproducts [19, 46]. Further evidences are inferred from the case of 44biPy, that sets an overpotential comparable to referential Py, but leads to r and FE values as low as those provided in absence of co-catalyst. Again, such efficiency lowering is attributable to a change in product selectivity as previously inferred from the anomalous peak observed in the voltammogram for 44biPy (Figure 3a).

Increase in pyridine concentration from 10 to 25 mM led to a noticeable lower CO_2 conversion performance. These results are unexpected according to the higher CO_2 reduction activity observed from cyclic voltammetric analyses (Figure 3b), but agree well with previous observations, where redox CO_2 reactions were found to be limited at high concentrations of Py. Apparently, as pointed in the previous section, availability of CO_2 is the limiting factor, in such a way that an excess of Py co-catalyst can induce the catalytic generation of H_2 [46], resulting in lower r and FE for CH_3OH. In particular, a recent report for the photocatalytic reduction of CO_2 in Ru-phenanthroline complex photosensitizers, concluded that when Py concentration was higher than 6.35 mM, another unidentified redox reaction, apart from the conversion of CO_2 to CH_3OH, took place [50]. Further increases in molecular catalyst concentration led to a drastic reduction in CH_3OH yield and *FE*, which can be explained by a combination of CO_2 and proton reduction, the latter process dominating as the concentration of pyridinium increased [18]. Overall, the results denoted the benefits of using a Cu_2O/ZnO-Py-based system with an optimum molecular catalyst concentration of 10 mM for the electroreduction of CO_2, although the results for CH_3OH concentration are limited to a sub-mg·L^{-1} level, irrespectively of the Py-based co-catalyst concentration.

In order to identify kinetic limitations for CH_3OH formation, Figure 4 presents the production rate and selectivity for CH_3OH formation in a current density range of *j*= 0.05 - 5 mA·cm^{-2} for the 2mPy (10 mM)-based system, where the best performance can be achieved.

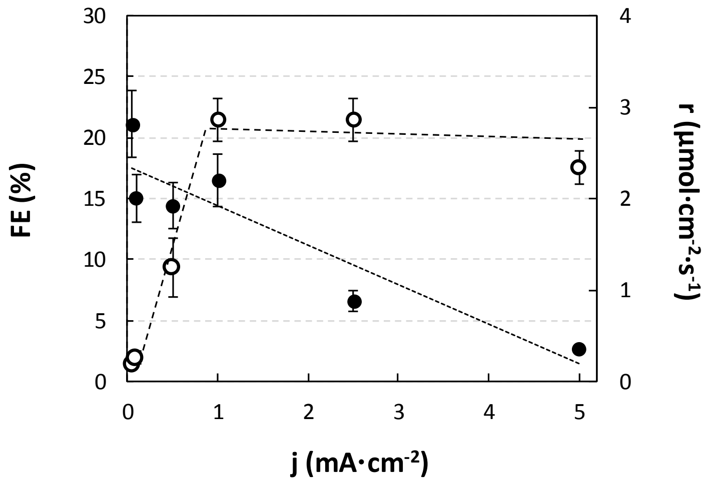

Figure 4. r(○) and *FE*(●) for Cu_2O/ZnO-2mPy (10 mM)-based system in a current density range of *j*= 0.05 - 5 mA·cm^{-2}.

The figure shows that *FE* for CH_3OH generally increased as the current density lowered. The same was observed by Barton et al. [21] and Frese et al. [51], where *FE* for CH_3OH increased as current density was reduced at Ga-based electrodes, due to the competing H_2 evolution in conjunction with CO_2 reduction. The same was recently reported by Rybchenko with Pt electrodes at high CO_2 pressure [27]. On the other hand, CH_3OH production rate is remarkably reduced at low current densities (*j*= 0.05 - 0.5 mA·cm^{-2}) but then remains almost invariable at increasing currents (*j*= 1 - 5 mA·cm^{-2}), indicating a reaction-limited rate. Overall, with 2mPy as soluble electrocatalyst and a semi-optimum current density of *j*= 1 mA·cm^{-2} the performance of the Py-co-catalyzed process seems to be enhanced.

3.3. Influence of pH and long-term stability

Previous literature demonstrated that CO_2 reduction is enhanced by pyridinum in aqueous solutions of pH ranging from 5.2 to 5.4 [19, 22, 23, 29, 47, 49, 52], which can be related to the pKa of Py [53]. It seems that at these pH conditions pyridinium exists in a higher concentration than the free proton, enabling the Py to function as proton source ($[PyH^+]$) as well as intermediates stabilizer via hydrogen bonding, enhancing also catalytic current [26, 30]. Table 2 shows the quantitative information (r and FE) regarding the production of CH_3OH at a pH ranging from 4 to 6 in the Cu_2O/ZnO-2mPy (10 mM) system. The pH was adjusted by adding HCl to the solution. Trace amounts of C_2H_5OH were also detected. The values are compared to the performance found at a pH of 7.6.

Table 2. r and FE at Cu_2O/ZnO-2mPy (10mM) for a pH range of 4 -7.6. j= 1 $mA\cdot cm^{-2}$. Q_e/A= 1 $ml\cdot min^{-1}\cdot cm^{-2}$, Q_g/A= 20 $ml\cdot min^{-1}\cdot cm^{-2}$

pH	E, V vs. Ag/AgCl	r, $\mu mol\cdot m^{-2}\cdot s^{-1}$	FE, %
7.6	-1.03	2.91	16.86
4	-0.59	2.18	12.65
5	-0.62	4.42	25.6
6	-0.84	3.28	18.97

As observed, a mild acidification (pH= 5-6) led to increases in CH_3OH production, indicating that reaction kinetics depend on the concentration of pyridinium ions ($[PyH^+]$) and/or hydrons available in the solution [26, 54, 55]. In fact, the marked lowering in the overpotential points to a change in the reaction mechanism which necessarily needs to go by a different transition state as the protonated pyridinium cannot directly form the carbamate [19]. Specifically, the rate for CH_3OH formation is as high as r= 4.42 $\mu mol\cdot m^{-2}\cdot s^{-1}$ at an optimum pH value of 5, which is around 1.5 times higher than the production rate observed for Cu_2O/ZnO-2mPy (10 mM) at pH=7.6. In the same manner, the efficiency of the process is significantly raised by reducing the pH of the solution, with a value as high as FE= 25.6% for an applied voltage of E= -0.62 V vs. Ag/AgCl (j= 1 $mA\cdot cm^{-2}$), thus corresponding to a overpotential of ca. 150 mV more than the thermodynamic potential needed for CH_3OH formation (-0.47 V vs. Ag/AgCl) at pH of 5.4 [22]. It is important to note that the reaction outcome improvement can be also attributed to the partial dissolution of ZnO at mild acidic pHs, which would render more

Cu_2O exposed at the surface of the cathode. It is also noteworthy to mention that this *FE* to CH_3OH formation is comparable to that maximum value obtained in our previous report for the same Cu_2O/ZnO-based catalyst in the absence of any Py molecular catalyst (FE_T= 27.5%) [12], although in this latter a current density of j= 10 mA·cm^{-2} was required. This indicates the relevance of using Py-based molecular catalysts to enhance the energy efficiency of the electrocatalytic reduction of CO_2.

Further reductions in pH to 4 produced a severe decrease in process efficiency, which could be initially interpreted by reductions in CO_2 solubility when decreasing the pH [18, 54]. Nonetheless, previous reports demonstrated the formation of copper(I) chloride (CuCl) in the presence of HCl when evaluating Cu-based electrocatalysts for CO_2 reduction [56]. CuCl compound has been proven to preferentially promote the formation of ethylene (C_2H_4) from the electrocatalytic reduction of CO_2, due to the ability of CuCl to reversibly combine with CO and C_2H_4 [56]. This will also explain the drastic reduction in *FE* to CH_3OH observed at pH= 4.

Finally, an evaluation of the Cu_2O/ZnO-2mPy (10 mM)-based system performance for CO_2 electroreduction at ambient conditions is evaluated in the long-run (5 h). The results for *r* and *FE* evolution are presented in Figure 5a and Figure 5b in a pH of 7.6 and 5, respectively. The stability of the co-catalyzed reduction was tracked while continuously sparging the solution with CO_2 at a constant current density of j= 1 mA·cm^{-2}, where a good balance between *FE* and *r* is observed (Figure 4, Table 1).

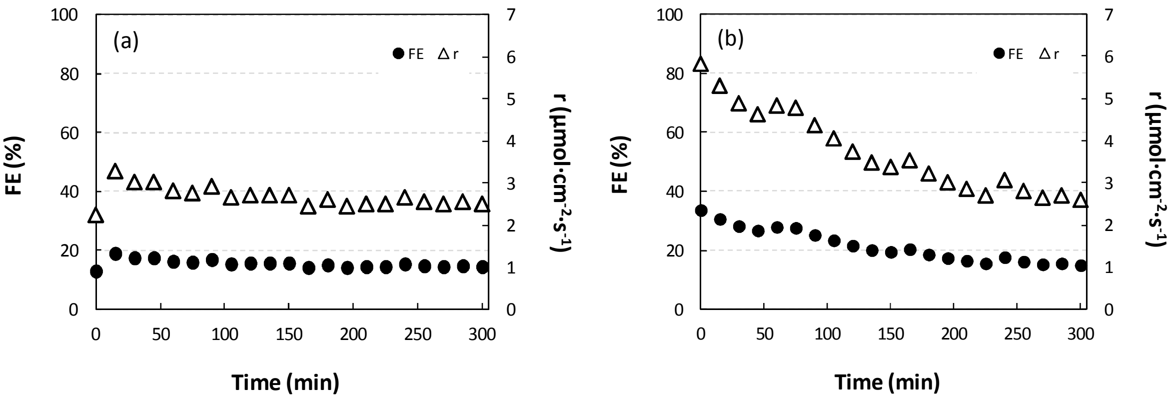

Figure 5. Time-dependence on *r* and *FE* for the Cu_2O/ZnO-2mPy (10 mM)-based system at (a) pH= 7.6 and (b) pH=5. j=1 mA·cm^{-2}, Q_e/A= 1 ml·min^{-1}·cm^{-2}, Q_g/A= 20 ml·min^{-1}·cm^{-2}.

As observed, the Cu_2O/ZnO-2mPy (10mM)-based system (pH= 7.6) showed only a slight activity decrease in the long run with a CH_3OH formation rate of r= 2.5 μmol·m^{-2}·s^{-1} and

FE= 14.45% at the end of the test (Figure 5a). We speculate that pairing a Py-based co-catalyst with a Cu_2O/ZnO cathode could potentially mitigate the limited stability observed in the electroreduction of CO_2 for CH_3OH production [9]. In fact, previous literature demonstrated that a stable electroreduction of CO_2 to HCOOH over 5 days can be reached at Sn-2mPy-based electrocatalytic system for a current applied of j= 1 $mA \cdot cm^{-2}$ in a membrane-separated cell [45]. In contrast, when the pH decreased to 5 (by the addition of HCl) a significant drop in process performance is clearly observed at the initial 3 h of experimental time with a 49% loss of activity (Figure 5b). Then, the production seems to slightly decrease (or stabilize) until the end of the test (r= 2.6 $\mu mol \cdot m^{-2} \cdot s^{-1}$, *FE*= 15.1%). In fact, the *FE* after 5 h is similar to that steady-state value observed for a pH = 7.6 (*FE*= 14.45%), which may probably indicate that the process performance is limited by the pyridine-Cu_2O/ZnO combination itself, rather than the pH of the electrolyte solution.

This reduction in process performance at pH= 5 is unexpected if we observe the stable CH_3OH formation rates reached at long reactions times in photo-and-electrocatalytic systems based on Ga, Pd and Ru metals at a similar pH level [21, 25, 26]. For example, Barton et al. found that the production of CH_3OH was linear with a charge passed ranging from 3 to 10 C at pH= 5.2 and 7 h of operation using a p-GaP-based photo-electrochemical cell. The Py concentration was also observed to be invariant over the time of the experiments, indicating that it is not consumed by the CH_3OH formation reaction [21]. In the same manner, Wang et al. [26] observed a stable production of CH_3OH, as solo product, from CO_2 in aid of Ru-phenanthroline complex photosensitizer. The yield of CH_3OH reached 60 $\mu mol \cdot L^{-1}$ after 6 h of reaction time. Literature shows, however, that certain metals, such as Zn [57] and Cu [58], corrode more easily and give up electrodes when exposed to an acidic solution, which lead to a reduced performance. From our analyses a striking feature is that cathodic voltage rose only slightly after 5 h of electrolysis, from -0.62 V (after 15 min.) to -0.76 V vs. Ag/AgCl to maintain a current density of j= 1 $mA \cdot cm^{-2}$ (Figure 5b). This limited increase in potential over time can be attributed to the consumption of the acid during the reduction process [47], since the pH of the aqueous electrolyte solutions increased from 5 to 5.69 after electrolysis. In any case, the limited increase in E probably indicate that the electrocatalytic system maintains its CO_2 reduction activity after 5 h of operation and thus, we hypothesized that the reduction in r and *FE* to CH_3OH observed has probably more to do with a variation in product selectivity (C_2H_4 formation with CuCl) [56], rather than the degradation of the catalytic material in the presence of HCl. Overall, the stable formation of CH_3OH at the Cu_2O/ZnO-2mPy (10 mM)-based system at a pH of 7.6, with a *FE*= 14.45% and moderate r= 2.5 $\mu mol \cdot m^{-2} \cdot s^{-1}$, show the potential of using Py-based molecular catalyst in the electroreduction of CO_2 to CH_3OH.

The outstanding scientific challenge seems to be in the understating of the underlying reaction mechanisms of Py-catalyzed CO_2 reduction processes to form CH_3OH, not only to exhaustively elucidate the role of Py but also to develop related catalysts that exploit the fundamental phenomena at play in the reduction reaction. It is suggested that the reduction mechanisms of the reduction proceed through various coordinative interactions between the Py radical and CO_2 to form carbamate-like species, which are proposed to be the rate determining step for the process [18, 59], and then a subsequent sequential electron and proton transfer processes to ultimately yield CH_3OH. In the current work, the inductive effect caused by the electron-withdrawing and releasing substituents on σ-donor N atom of the Py ring seems to play an important role in the electron transfer to CO_2 and thus, in the reaction outcome. However, there is a delicate balance between kinetics and thermodynamics underlying the observed reactivity. While increased electron-releasing ability of the Py-based molecular catalyst is predicted to favour the electron transfer to the electrophilic C atom of the CO_2 and increase reaction rate corresponding to this stage, at the same time this would also stabilize the carbamate species, which is not desired for the subsequent CH_3OH formation [18]. Certainly, further experimental work is required to fully elucidate CO_2 reduction steps to CH_3OH in the Py-based catalysed reaction, including the analysis of charge-transfer proccesses and the governing physical and chemical phenomena taking place in the electrochemical systems [60], although significant research efforts have been recently made [16, 26, 30-32, 54, 61-66].

4. Conclusions

This work demonstrated the beneficial use of pyridine-based molecular catalysts containing electron-releasing or electron-withdrawing groups (i.e. 2-methylpyridine, 4-ethylpyridine, 2,4,6-trimethylpyridine, pyridine, 2-chloropyridine, 4,4-bipyridine), to reach enhanced energy efficiencies for the electrocatalytic reduction of CO_2 to methanol at Cu_2O/ZnO-based surfaces.

The results showed that all the applied pyridine-based soluble co-catalysts lowered the overpotential for the electrochemical reduction of CO_2. In particular, the reduction response occurred at around 200 mV lower overpotential in the presence of 2-methylpyridine (compared to the electrocatalytic system with a CO_2-saturated electrolyte without it). The overpotential reduction with respect to the unsubstituted Py is explained by electron-releasing alkyl groups (*I+ effect*) that makes the pyridinic ring more prone to transfer an electron through a nucleophilic addition and consequent formation of a carbamate intermediate.

The continuous electroreduction of CO_2 to methanol tests in a filter-press electrochemical cell, showed a maximum methanol formation rate when using 2-methylpyridine (10 mM), r= 2.91 $\mu mol \cdot m^{-2} \cdot s^{-1}$ (Faradaic efficiency= 16.86%), which is significantly higher than that value in the absence of any molecular catalyst, r= 0.21 $\mu mol \cdot m^{-2} \cdot s^{-1}$ (Faradaic efficiency= 1.2%). Importantly, process efficiency was significantly raised by reducing the pH of the electrolyte to 5, with Faradaic efficiencies as high as FE= 25.6% for an applied voltage of E= -0.62 V vs. Ag/AgCl (j= 1 $mA \cdot cm^{-2}$) in the 2mPy (10 mM)-based system. This system, however, showed deactivation at longer reaction times, which may be associated to a change in the selectivity of the reaction (i.e. formation of ethylene).

Acknowledgements

The authors gratefully acknowledge the financial support from the Spanish Ministry of Economy and Competitiveness (MINECO), under the projects CTQ2013-48280-C3-1-R, CTQ2014-55716-REDT and Juan de la Cierva program (JCI-2012-12073).

References

[1] Albo J., Yoshioka T., Tsuru T., Porous Al_2O_3/TiO_2 tubes in combination with 1-ethyl-3-methylimidazolium acetate ionic liquid for CO_2/N_2 separation. Sep. Purif. Technol. 122 (2014) 440-448.

[2] Albo J., Irabien A., Non-dispersive absorption of CO_2 in parallel and cross-flow membrane modules using EMISE. J. Chem. Technol. Biot. 87:10 (2012) 1502-1507.

[3] Albo J., Luis P., Irabien A. Carbon dioxide capture from flue gases using a cross-flow membrane contactor and the ionic liquid 1-ethyl-3-methylimidazolium ethylsulfate. Ind. Eng. Chem. Res. 49:21 (2010) 11045-11051.

[4] International Energy Agency (IEA). (2015). CO_2 emissions from fuel combustion: Highlights.

[5] Aresta M., Dibenedetto A., Angelini A., Catalysis for the valorization of exhaust carbon: From CO_2 to chemicals, materials, and fuels. Technological use of CO_2. Chem. Rev. 114 (2014) 1709-1742.

[6] Centi G., S. Perathoner S., Opportunities and prospects in the chemical recycling of carbon dioxide to fuels. Catal. Today. 148 (2009) 191-205.

[7] Martín A. J., Larrazábal G. O., Pérez-Ramírez J., Towards sustainable fuels and chemicals through the electrochemical reduction of CO_2: lessons from water electrolysis. Green Chem. 17 (2015) 5114-5130.

[8] Dominguez-Ramos A., Singh B., Zhang X., Hertwich E. G., Irabien A., Global warming footprint of the electrochemical reduction of carbon dioxide to formate. J. Cleaner Prod.104 (2015) 148-155.

[9] Albo J., Alvarez-Guerra M., Castaño P., Irabien A., Towards the electrochemical conversion of carbon dioxide into methanol. Green Chem. 17 (2015) 2304-2324.

[10] Olah G. A., Goeppert A., Prakash G. K. S., Beyond oil and gas: the methanol economy. Wiley-VCH, Weinheim, 2006.

[11] Albo J., Vallejo D., Beobide G., Castaño P., Cu-based metal-organic porous materials for CO_2 electroreduction to alcohols. ChemSusChem. (2016). doi: 10.1002/cssc.201600693.

[12] Albo J., Irabien A., Cu_2O-based catalysts for the electrochemical reduction of CO_2 at gas-diffusion electrodes. J. Catal. 343 (2016) 232-239.

[13] Albo J., Sáez A., Solla-Gullón J., Irabien A., Production of methanol from CO_2 electroreduction at Cu_2O and Cu_2O/ZnO-based electrodes in aqueous solution. Appl. Catal. B-Environ. 176-177 (2015) 709-717.

[14] Lim R. J., Xie M., Ska M. A., Leea J-M., Fisher A., Wang X., Lim K. H. A review on the electrochemical reduction of CO_2 in fuel cells, metalelectrodes and molecular catalysts. Catal. Today. 233 (2014) 169-180.

[15] Oha Y., W. A. Organic molecules as mediators and catalysts for photocatalytic and electrocatalytic CO_2 reduction. Chem. Soc. Rev. 42 (2013) 2253-2261.

[16] Yan Y., Zeitler E. L., Gu J., Hu Y., Bocarsly A. B., Electrochemistry of aqueous pyridinium: exploration of a key aspect of electrocatalytic reduction of carbon dioxide to methanol. J. Am.Chem. Soc. 135 (2013) 14020-14023.

[17] Bocarsly A. B., Gibson Q. D., Morris A. J., L'Esperance R. P., Detweiler Z. M., Lakkaraju P. S., Zeitler E. L. Shaw T. W., Comparative study of imidazole and pyridine catalyzed reduction of carbon dioxide at illuminated iron pyrite electrodes, ACS Catal. 2 (2012) 1684-1692.

[18] Morris A. J., McGibbon R. T., Bocarsly A. B., Electrocatalytic carbon dioxide activation: the rate-determining step of pyridinium-catalyzed CO_2 reduction. ChemSusChem. 4 :2 (2011) 191-196.

[19] Barton C. E., Lakkaraju P. S., Rampulla D. M., Morris, A. J., Abelev, E., Bocarsly, A. B., Using a one-electron shuttle for the multielectron reduction of CO_2 to methanol: kinetic, mechanistic, and structural insights, J. Am. Chem. Soc. 132: 33 (2010) 11539-11551.

[20] Rosen B. A., Salehi-Khojin A., Thorson M. R., Zhu W., Whipple D. T., Kenis P. J. A., Masel R. I., Ionic liquid–mediated selective conversion of CO_2 to CO at low overpotentials, Science. 74: 2 (2009) 487-498.

[21] Barton C. E., Rampulla D. M., Bocarsly A. B., Selective solar-driven reduction of CO_2 to methanol using a catalyzed p-GaP based photoelectrochemical cell, J. Am. Chem. Soc. 130 (2008) 6342-6344.

[22] Seshadri G., Lin C., Bocarsly A. B., A new homogeneous electrocatalyst for the reduction of carbon dioxide to methanol at low overpotential, J. Electroanal. Chem. 372: 1-2 (1994) 145-150.

[23] Boston D. J., Xu C., Armstrong D. W., MacDonnell F. M., Photochemical reduction of carbon dioxide to methanol and formate in a homogeneous system with pyridinium catalysts. J. Am. Chem. Soc. 135: 44 (2013)16252-16255.

[24] Dongmei X., Magana D., Dyer R. B., CO_2 reduction catalyzed by mercaptopteridine on glassy carbon. J. Am. Chem. Soc. 2014, 136:40 (2014)14007-14010.

[25] Yang H., Qin S., Wang H., Lu J., Organically doped palladium: a highly efficient catalyst for electroreduction of CO_2 to methanol. Green Chem. 17 (2015) 5144-5148.

[26] Wang W., Zhang J., Wang H., Chen L., Bian Z., Photocatalytic and electrocatalytic reduction of CO_2 to methanol by the homogeneous pyridine-based systems. Appl. Catal. A-Gen. 520 (2016) 1-6.

[27] Rybchenko S., Touhami D., Wadhawan J, Haywood S., Study of Pyridine-Mediated Electrochemical Reduction of CO_2 to Methanol at High CO_2 Pressure. ChemSusChem. 9:13 (2016) 1660-1669.

[28] Yang H., Qin S., Yue Y., Liu L., Wang H., Lu J. Entrapment of a pyridine derivative within copper-palladium alloy: a bifunctional catalyst for electrochemical reduction of CO_2 to alcohols with excellent selectivity and reusability. Catal. Sci. Technol. 6 (2016) 6490-6494.

[29] Yang H., Yue Y., Qin S., Wang H., Lu J., Selective electrochemical reduction of CO_2 to different alcohol products by an organically doped alloy catalyst. Green Chem. 18 (2016) 3216-3220.

[30] Ertem M. Z., Konezny S. J., Araujo C. M., Batista V. S., Functional Role of Pyridinium during Aqueous Electrochemical Reduction of CO2 on Pt(111). J. Phys. Chem. Lett. 4: 5 (2013) 745-748.

[31] Lim C. H., Holder A. M., Musgrave C. B., Mechanism of homogeneous reduction of CO_2 by pyridine: proton relay in aqueous solvent and aromatic stabilization. J. Am. Chem. Soc. 135 (2013) 142-154.

[32] Keith J. A., Carter E. A., Theoretical insights into pyridinium-based photoelectrocatalytic reduction of CO_2. J. Am. Chem. Soc. 134: 18 (2013) 7580-7583.

[33] Keith J. A., Carter E. A., Electrochemical reactivities of pyridinium in solution: consequences for CO_2 reduction mechanisms. Chem. Sci. 4 (2013) 1490-1496.

[34] Yasukouchi K., Taniguchi I., Yamaguchi H., Shiraishi M. J., Cathodic reduction of pyridinium ion in acetonitrile. J. Electroanal. Chem. 105 (1979) 403-408.

[35] Qiao J., Liu Y., Hong F., Zhang J., A review of catalysts for the electroreduction of carbon dioxide to produce low-carbon fuels. Chem. Soc. Rev. 43 (2014) 631-675.

[36] Peterson A. A., Abild-Pedersen F., Studt F., Rossmeisl J., Nørskov J. K., How copper catalyzes the electroreduction of carbon dioxide into hydrocarbon fuels, Energy Environ. Sci. 3 (2010) 1311-1315.

[37] Gattrell M., Gupta N., Co A., A review of the aqueous electrochemical reduction of CO_2 to hydrocarbons at copper. J. Electroanal. Chem. 594 (2006) 1-19.

[38] Kuhl K. P., Cave E. R., Abram D. N., Jaramillo T. F., New insights into the electrochemical reduction of carbon dioxide on metallic copper surfaces. Energy Environ. Sci. 5 (2012) 7050-7059.

[39] Aeshala L. M., Uppaluri R. G., Verma A., Effect of cationic and anionic solid polymer electrolyte on direct electrochemical reduction of gaseous CO_2 to fuel. J. CO_2 Util. 3-4 (2013) 49-55.

[40] Le M, Ren M., Zhang Z., Sprunger P. T., Kurtz R. L., Flake J. C., Electrochemical Reduction of CO_2 to CH_3OH at copper oxide surfaces. J. Electrochem. Soc.158: 5 (2011) E45-E49.

[41] Frese K. W., Electrochemical reduction of CO_2 at intentionally oxidized copper electrodes. J. Electrochem. Soc. 138: 11 (1991) 3333-3344.

[42] Heinzel A., Barragan V. M., A review of the state-of-the-art of the methanol crossover in direct methanol fuel cells. J. Power Sources. 84:1 (1999) 70-74.

[43] Del Castillo A., Alvarez-Guerra M., Irabien A., Continuous electroreduction of CO_2 to formate using Sn gas diffusion electrodes. AIChE J. 60:10 (2014) 3557-3564.

[44] Merino-García I., Alvarez-Guerra E., Albo J., Irabien A., Electrochemical membrane reactors for the utilisation of carbon dioxide. Chem. Eng. J. 305:1 (2016) 104-120.

[45] Parajuli R., Gerken J. B., Keyshar K., Sullivan I., Sivasankar N., Teamy K., Stahl S. S., Barton C. E., Integration of anodic and cathodic catalysts of earth abundant materials for efficient, scalable CO_2 reduction. Top. Catal. 58:1 (2015) 57-66.

[46] Baumgartel H., Retzlav K. J., Heteroaromatic Compounds. In Encyclopedia of Electrochemistry of the Elements; Bard A. J., Lund H., Eds.; Marcel Dekker: New York, 1984; Vol. XV, p 194.

[47] Lee H. Q. J., Lauw S. J. L., Webster R. D., The electrochemical reduction of carbon dioxide (CO_2) to methanol in the presence of pyridoxine (vitamin B6). Electrochem. Commun. 64 (2016) 69-73.

[48] Cole E. E. B., Baruch M. F., L'Esperance R. P. L., Kelly M. T., Lakkaraju P. S., Zeitler E. L., Bocarsly A. B., Substituent effects in the pyridinium catalyzed reduction of CO_2 to methanol: further mechanistic insights. Top. Catal. 58 (2015) 15-22.

[49] Portenkirchner E., Enengl C., Enengl S., Hinterberger G., Schlager S., Apaydin D., Neugebauer H., Knör G., Sariciftci N. S., A comparison of pyridazine and pyridine as electrocatalysts for the reduction of carbon dioxide to methanol. ChemElectroChem. 1 (2014) 1543-1548.

[50] Ponnurangam S., Yun C. M., Chernyshova I. V., Robust electroreduction of CO_2 at a poly(4-vinylpyridine)-copper Electrode. ChemElectroChem. 3 (2016) 74-82.

[51] Frese K. W., Canfield D., Reduction of CO_2 on n-GaAs electrodes and selective methanol synthesis. J. Electrochem. Soc. 131:11 (1984) 2518-2522.

[52] Lebégue E., Agullo J., Morin M., Bélanguer D., The role of surface atoms in the electrochemical reduction of pyridine and CO_2 in aqueous electrolyte. ChemElectroChem. 1 (2014) 1013-1017.

[53] Hanai T., Koizumi K., Kinoshita T., Arora R., Ahmed F., Prediction of pKa values of phenolic and nitrogen-containing compounds by computational chemical analysis compared to those measured by liquid chromtography. J. Chromatogr. A. 762 (1997) 55-61.

[54] Yuan J., Hao C., Solar-driven photoelectrochemical reduction of carbon dioxide to methanol at $CuInS_2$ thin film photocathode. Sol. Energ. Mat. Sol. C. 108 (2013) 170-174.

[55] Appel A. M., Bercaw J. E., Bocarsly A. B., Dobbek H., DuBois D. L., Dupuis M., Ferry J. G., Fujita E., Hille R., Kenis P. J. A., Kerfeld C. A., Morris R. H., Peden C. H. F., Portis A. R., Ragsdale S. W., Rauchfuss T. B., Reek J. N. H., Seefeldt L. C., Thauer

R. K., Waldrop G. L., Frontiers, opportunities, and challenges in biochemical and chemical catalysis of CO_2 fixation. Chem. Rev. 113 (2013) 6621-6658.

[56] Ogura K., Yano H., Shirai F., Catalytic reduction of CO_2 to ethylene by electrolysis at a three-phase interface. J. Electrochem. Soc. 150(9) (2003) D163-D168.

[57] Qi J., Zhang K., Ji Z., Xu M., Wang Z., Zhang Y., Dissolving behavior and electrical properties of ZnO wire in HCl solution. RSC Adv. 5 (2015) 44563-44566.

[58] Sherif E-S. M., Corrosion behavior of copper in 0.50 M hydrochloric acid pickling solutions and its inhibition by 3-amino-1,2,4-triazole and 3-amino-5-mercapto-1,2,4-triazole. Int. J. Electrochem. Sci. 7 (2012) 1884-1897.

[59] Kamrath M. Z., Relph R. A., Johnson M. A., Vibrational predissociation spectrum of the carbamate radical anion, $C_5H_5N\text{-}CO_2^-$, generated by reaction of pyridine with $(CO_2)_m^-$. J. Am. Chem. Soc. 132 (2010) 15508-15511.

[60] Ehsani A., Mahjani M.G., Jafarian M., Naeemy A., Electrosynthesis of polypyrrole composite film and electrocatalytic oxidation of ethanol. Electrochim. Acta. 71 (2012) 128-133.

[61] Lim C-H., Holder A. M., Hynes J. T., Musgrave C. B., Reduction of CO_2 to methanol catalyzed by a biomimetic organo-hydride produced from pyridine. J. Am. Chem. Soc. 136 (2014) 16081-16095.

[62] Keith J. A., Carter E. A., Theoretical insights into electrochemical CO_2 reduction mechanisms catalyzed by surface-bound nitrogen heterocycles. J. Phys. Chem. Lett. 4 (2013) 4058-4063.

[63] Costentin C., Canales J. C., Haddou B., Saveant J. M., Electrochemistry of acids on platinum. Application to the reduction of carbon dioxide in the presence of pyridinium ion in water. J. Am. Chem. Soc. 135 (2013) 17671-17674.

[64] Lessio M., Cartes E. A., What is the role of pyridinium in pyridine-catalyzed CO_2 reduction on p-GaP photocathodes? J. Am. Chem. Soc. 137 (2015) 13248-13251.

[65] Senftle T., Lessio M., Carter E., Interaction of pyridine and water with the reconstructed surfaces of GaP(111) and CdTe(111) photoelectrodes: Implications for CO_2 reduction. Chem. Mater. 28:16 (2016) 5799-5810.

[66] Schneider T., Ertem M., Muckerman J., Angeles-Boza A., Mechanism of Photocatalytic Reduction of CO_2 by Re(bpy)$(CO)_3$Cl from Differences in Carbon Isotope Discrimination. ACS Catal. 6 (2016) 5473-5481.